Thermal Properties of D0 Run IIB Silicon Detector Staves

Giobatta Lanfranco and James Fast

Fermi National Accelerator Laboratory
Particle Physics Division /Mechanical Dep. - Silicon Engineering Group
e-mail: giobatta@fnal.gov, jfast@fnal.gov

14 June 2001

1. Abstract

A proposed stave design for the D0 Run IIb silicon tracker outer layers featuring central cooling channels and hybrid substrates mounted directly to the silicon sensor surfaces is evaluated for heat transfer characteristics and thermal deflections. In order to control leakage current noise in the silicon it is necessary to maintain the silicon in Layer 2 (R~100mm) at or below +5C. The current cooling system using 30% ethylene glycol in water can deliver coolant to the inlet of the silicon tracker at a temperature of –8C to –10C. This paper also investigates some alternative coolant options for Run IIB. While these are not required for the outer layers of silicon, they may be needed for L0, which sits at R~15mm. In this case the silicon must be kept at or below –5C, very near the lower limit for delivery of 30% glycol/water coolant. However, for the inner layers the electronics will be mounted independently from the silicon so the local heat flux is greatly reduced. This paper does not consider the cooling issues for the inner layers.

2. The Stave Design

The stave is constructed from 200mm long ladders consisting of two silicon sensors, 37.2 mm wide by 100 mm long, glued together end-to-end with a hybrid, 35 mm wide and 60 mm long, glued to the silicon, centered on the sensor to sensor joint. Six of these ladder structures are joined end-to-end to form a 1.2m long chain and two chains are attached to opposite sides of the stave core and cooling lines. Each hybrid has 10 SVX chips mounted on it for a total heat load of 5W per hybrid. Figure 1 shows a cross-section of the stave. Table 1 summarizes the stave constituent materials, their thickness and their thermal conductivities.

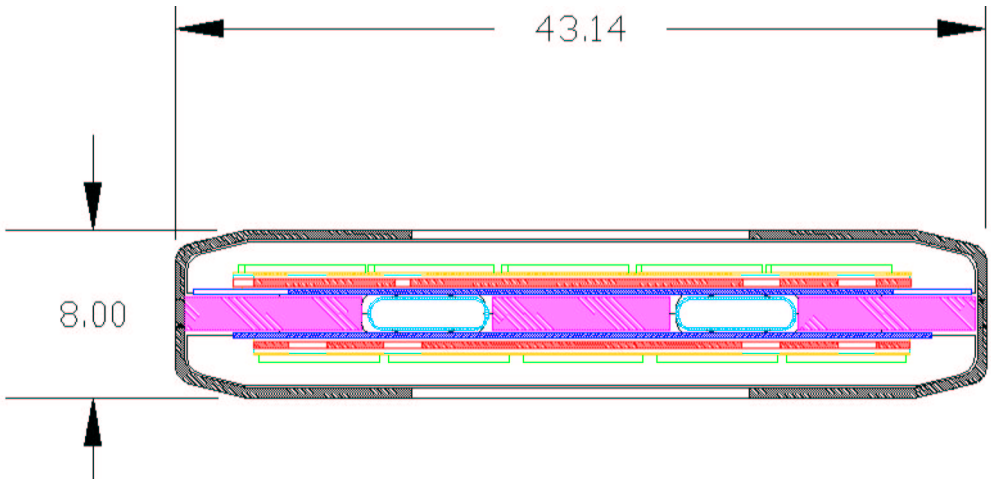

Figure 1 – The stave cross section

Component	material	Thickness [μm]	Thermal conductivity [W/mK]	Color in Figure 1
Support Shell	Carbon Fiber K139	500	25-80 in-plane 0.4 inter-plane	black
Sensor	Silicon	380	124	blue
Chip	Silicon	300	124	green
Glue	Epoxy	50	1	white
Tubing type 1	Al 1100	100	222	cyan
Tubing type 2	PEEK	100	0.25	cyan
HDI	Kapton	100	0.2	gold
Substrate	BeO	500	250	red
Heat spreader Type 1	TPG	100	600-800 in-plane 5 inter-plane	not shown
Heat spreader Type 2	Carbon Fiber K13D2U	100 (3 plies x 33 μm)	150-300 in-plane 0.3 inter-plane	not shown
Heat spreader Type 3	Kapton	50	0.2	not shown

Table 1 – Thermal conductivities and thickness of the stave constituent materials

3. The Finite Element Model

The governing law of heat conduction is the *Laplace equation*, a second-order ordinary differential equation. For one-dimensional, steady state conduction the temperature distribution can't be determined unless two boundary conditions are specified.

The heat generated in the chip sets the first condition. The chip size used in the model is 11.6 mm long by 6.4 mm wide, each chip dissipating 0.5W. The heat generation is not homogeneously distributed: 25% of the power is dissipated along 2 mm wide strips at each end of the 11.6 mm dimension, while the remaining 50% is dissipated in the central region.

The second condition is set through the convection at the inner wall of the cooling pipe. The second part of this paper contains a study of some of the feasible coolants, which will let us predict the achievable average bulk temperature in the pipe along with the film coefficient. For simplicity, the problem can be split into two parts, with the finite element analysis providing the thermal gradient along the stave and the theoretical analysis of the coolant fixing the temperature drop from the tube wall to the bulk fluid. In the finite element model the bulk temperature of the coolant has been fixed at –5 °C and a convection film coefficient h_c=2000 W/m^{2}K is used.

To reduce the calculations required, observing the longitudinal symmetry, only one quarter of the stave has been considered. This is reflected in the pictures shown (Figure 3 through Figure 8).

Figure 2 – Detail of the stave material stuck-up. Colour guide: violet – Silicon (chip, detector); pink – kapton (hdi); azure – beryllia oxide (substrate); orange – TPG/K13D2U/Kapton layer; aqua – epoxy; red – PEEK(tubing)

3.1. Finite Element Analysis Results

Six different configurations have been studied. Aluminium tubing, although providing the best performance from a thermal standpoint, is subject to galvanic corrosion when in contact with carbon fiber as well as to the risk of erosion due to the ions in the coolant. These problems, together with a non

optimal radiation length, make it necessary to investigate alternative materials. PEEK (Polyetheretherketone), even though it has a very low thermal conductivity, has none of the problems affecting aluminium, it is radiation hard and its low modulus of elasticity can be an advantage when the tube is coupled to the silicon sensors. Configurations 1 and 2 compare aluminium with PEEK tubing. An attempt to improve the poorer PEEK thermal performance is studied in configuration 3; even though a TPG (Thermal Pyrolytic Graphite) hybrid substrate is not viable because of the intrinsic manufacturing limitations, use of a higher thermal conductivity material in the hybrid substrate can effectively reduce the temperature in the detector.

Finally, configurations 4, 5 and 6 analyze the effect of an extra layer of TPG, high conductivity carbon fiber or Kapton added between the stave core (cooling lines) and the sensors. This layer would greatly aid stave assembly by making the core structure a mechanically stable sub-assembly prior to attachment of the silicon ladders. The better TPG performance may not justify the higher cost of the material and the lower mechanical performance when compared with the K13D2U laminate. The Kapton layer is considered for electrical insulation purposes. Its good results, even if apparently in contradiction with its low thermal conductivity, may be explained by its lower thickness together with the fact that in all the three configurations the conductivity of the materials through the plane are comparable and rather low.

	Configuration	**$T_{max\ chip}$ [°C]**	**$T_{max\ silicon}$ [°C]**
1	*Aluminium Tubing*	2.2	-1.6
2	*PEEK Tubing*	4.5	0.8
3	*PEEK Tubing + TPG substrate*	3.4	-0.7
4	*PEEK Tubing with TPG layer*	4.0	0.2
5	*PEEK Tubing with K13D2U layer*	5.2	1.5
6	*PEEK Tubing with Kapton layer**	3.9	-0.2

Table 2 – Finite element configurations and maximum temperature on the SVX chips and in the silicon sensors. Unless specified, a BeO substrate is used. (note that the Kapton layer is 50μm thick, vs. 100μm for the other materials)*

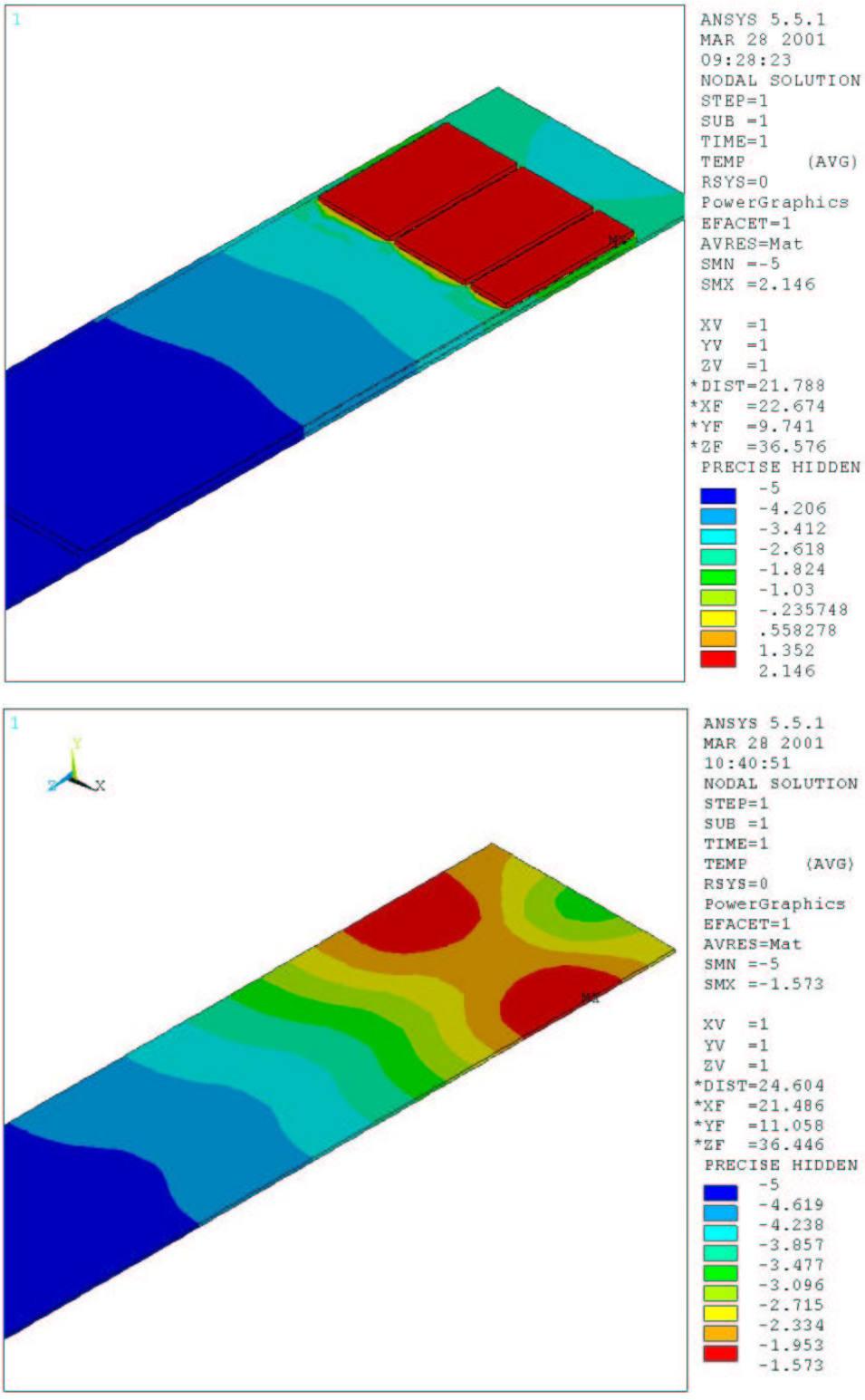

Figure 3 – Temperature distribution of the silicon ladder with aluminum cooling tubing.

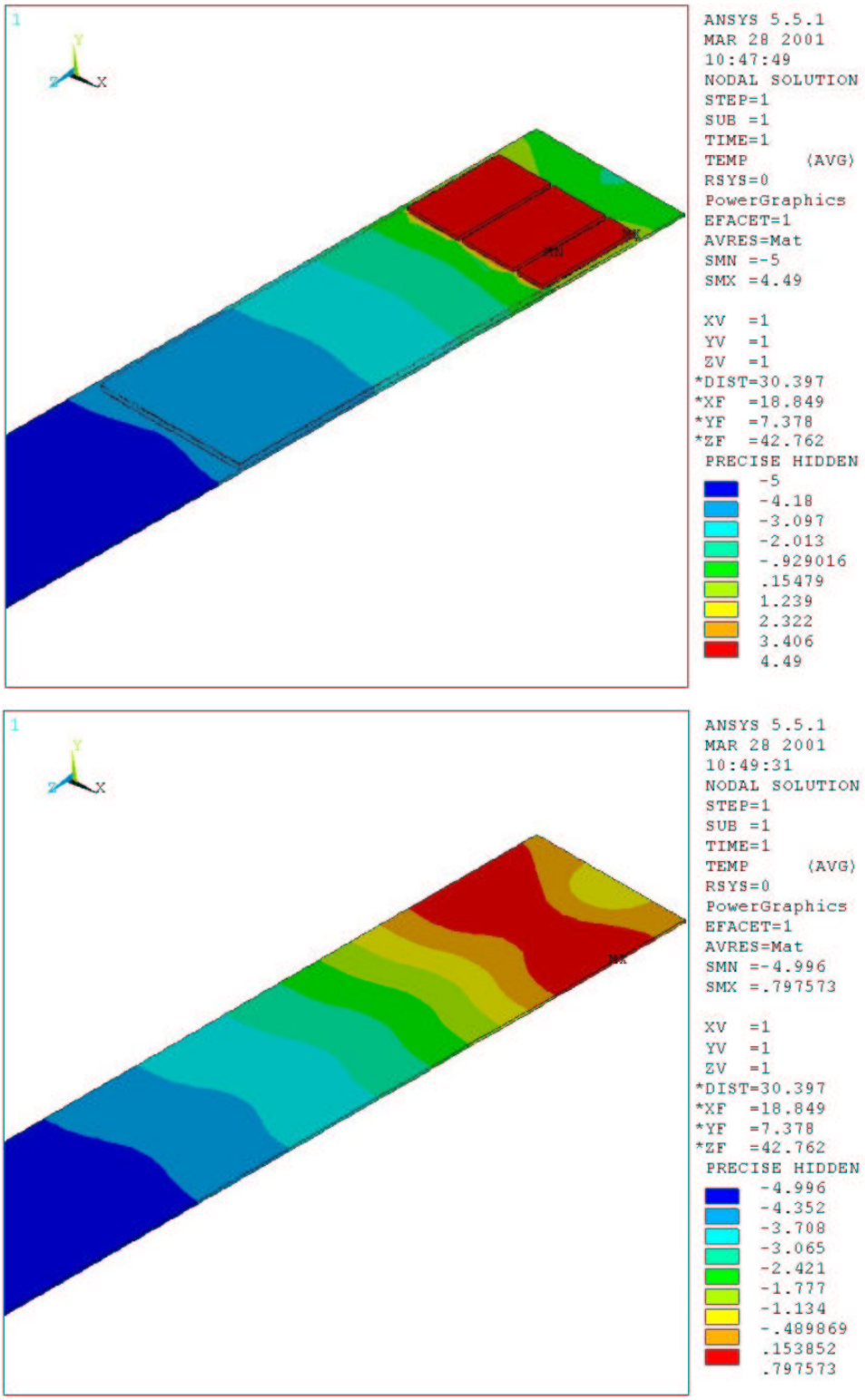

Figure 4 - Temperature distribution of the silicon ladder with PEEK cooling tubing.

The upper plot shows the ladder with hybrid while the lower plot shows the temperature distribution in the silicon sensor.

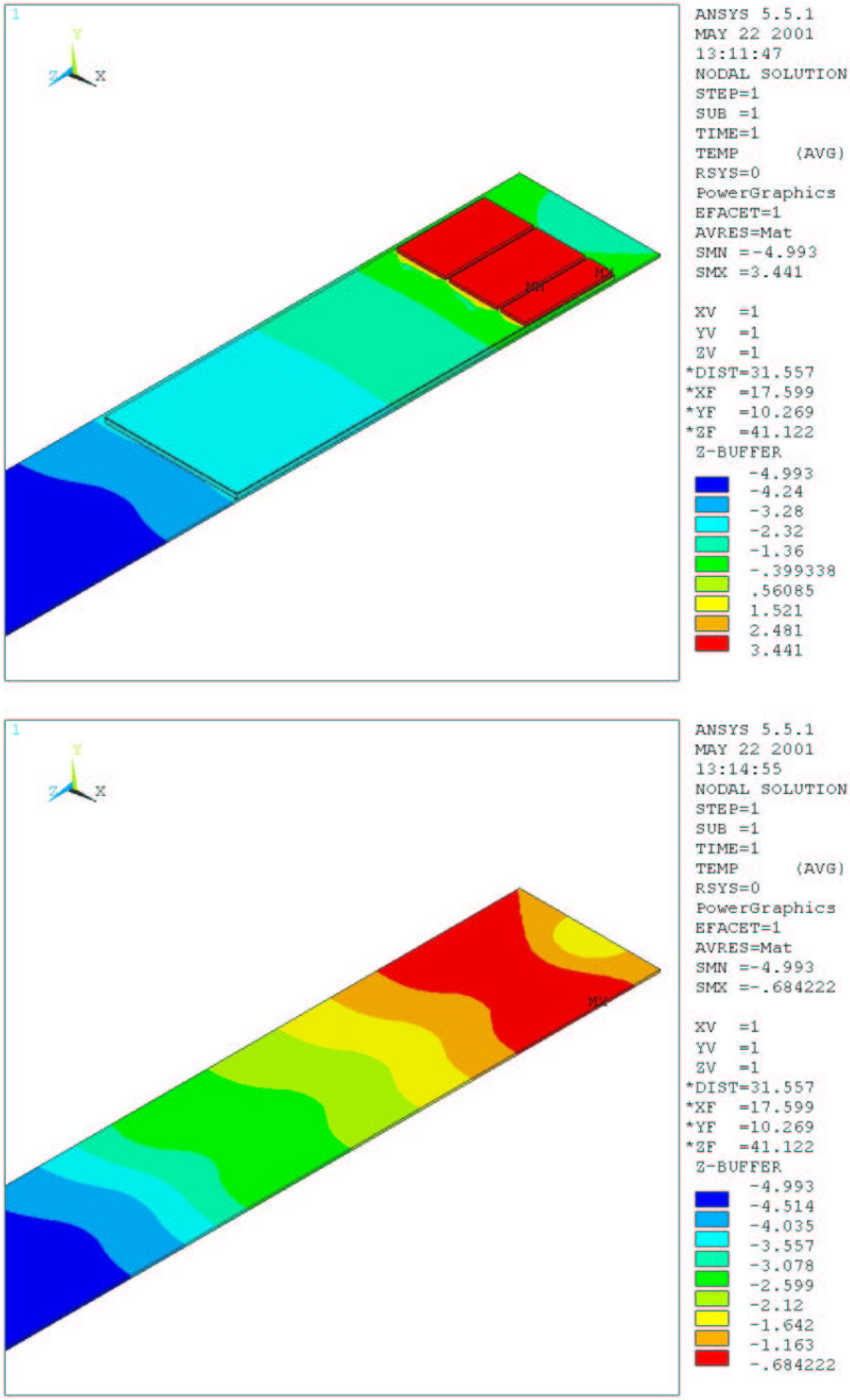

Figure 5 - Temperature distribution of the silicon ladder with PEEK cooling tubing and TPG substrate.

The upper plot shows the ladder with hybrid while the lower plot shows the temperature distribution in the silicon sensor.

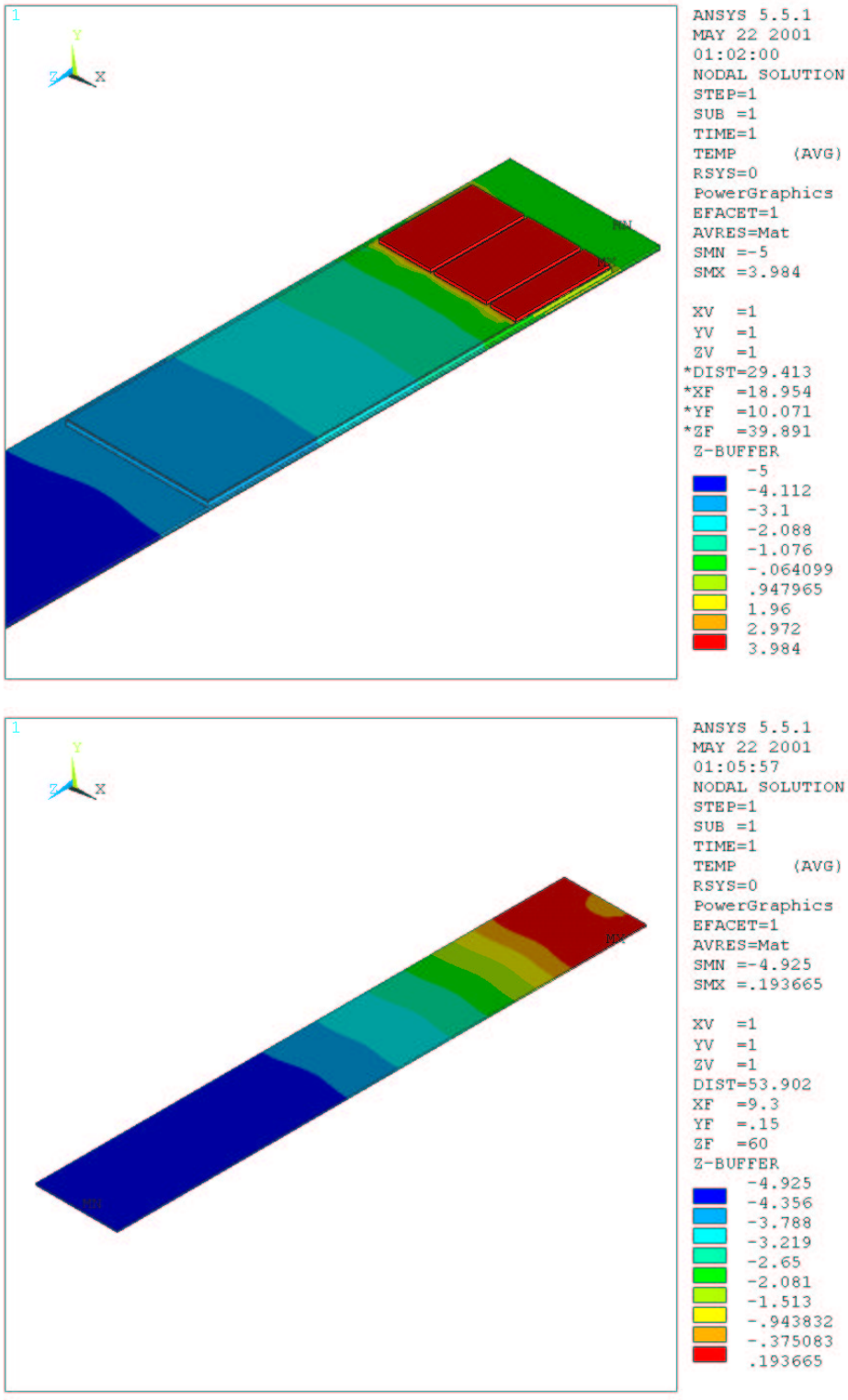

Figure 6 - Temperature distribution of the silicon detector with PEEK cooling tubing and TPG layer.

The upper plot shows the ladder with hybrid while the lower plot shows the temperature distribution in the silicon sensor.

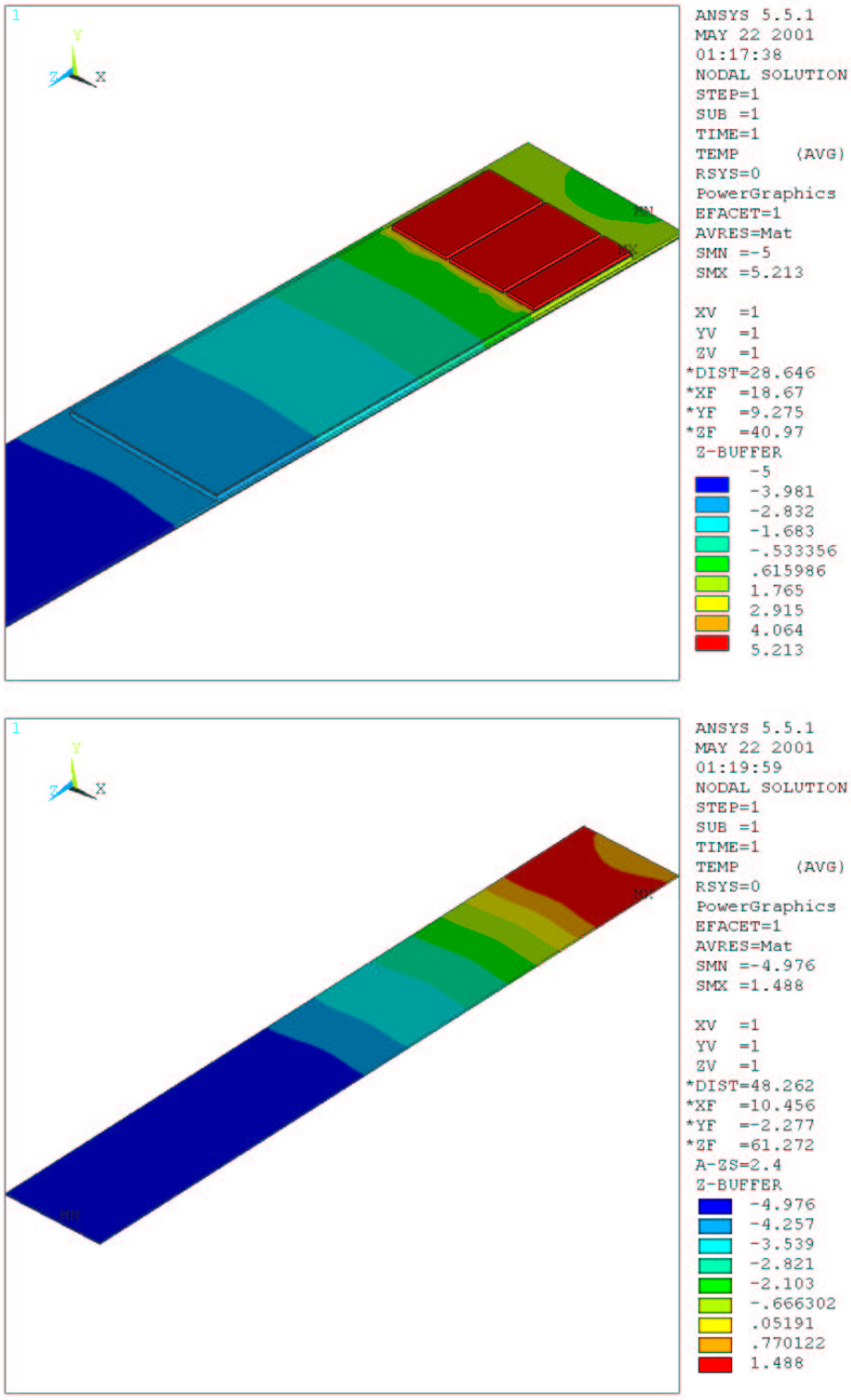

Figure 7 - Temperature distribution of the silicon detector with PEEK cooling tubing and K13D2U layer.

The upper plot shows the ladder with hybrid while the lower plot shows the temperature distribution in the silicon sensor.

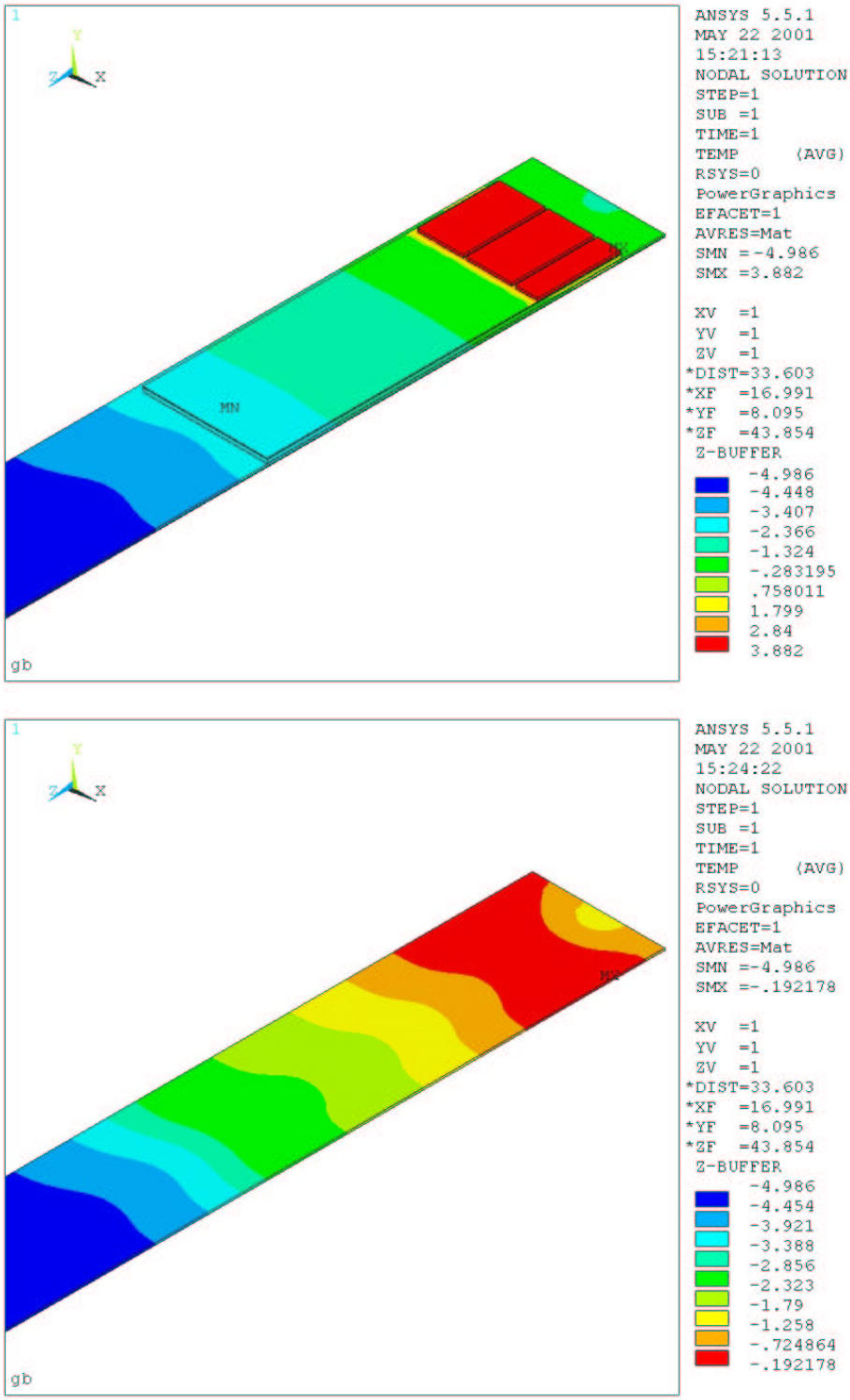

Figure 8 - Temperature distribution of the silicon detector with PEEK cooling tubing and Kapton layer.

The upper plot shows the ladder with hybrid while the lower plot shows the temperature distribution in the silicon sensor.

4. Coolant Performance Analysis

In order to evaluate and compare the performance offered by some of the most promising coolants nowadays widely adopted in cooling systems, the flow in a 1.2 m long pipe has been investigated. The pipe has a rectangular section and the outer dimensions are 6 mm by 2 mm; the wall thickness is 100μm. Given a power of 100 W to dissipate and given a flow bulk temperature at the entrance T_{b1} = 263 K, two different conditions at the pipe exit have been set:

1. bulk temperature T_{b2} = 265 K;
2. pressure drop in the conduit ΔP = 6 psi

The cooling efficiency has been evaluated comparing the flow speed U reached in the pipe, the mass rate M required for the heat transfer, the average wall temperature T_{wall}, the film coefficient h_c and the following dimensionless numbers:

- *Reynolds number*

$$\mathrm{Re} = \frac{\rho U D_H}{\mu}$$

where ρ is the density, *U* the velocity, D_H the hydraulic diameter and μ the fluid viscosity. Re relates the viscous and inertial forces and determines the transition from laminar to turbulent flow. For flow in long ducts, where the entrance effects are not important, the laminar region ends around Re = 2320; from 2320 to 10000 a transition from laminar to turbulent flow takes place, where the viscous effects become more and more important (*transitional regime*); after that the turbulent flow is completely developed.

- *Nusselt number*

$$\mathrm{Nu} = \frac{h_c D_H}{k}$$

where *k* is the thermal conductivity; Nu, relating the film coefficient to the thermal conductivity of the fluid, gives an indication of which heat transfer phenomenon – convection versus conduction – is prevailing in the fluid and provides a direct way to calculate h_c.

- *Prandtl number*

$$\mathrm{Pr} = \frac{\nu}{\alpha} = \frac{c_p \mu}{k}$$

where ν is the kinematic viscosity, α the thermal diffusivity and c_p the specific heat. Since ν can be seen as the molecular diffusivity of momentum, Pr relates the temperature distribution to the

velocity distribution. So the temperature gradient at the wall will be steeper in a fluid having a large Prandtl number at a specified Re. Consequently also the Nu will be larger and the convection will be more efficient.

The aforementioned quantities can be interpreted as follows:

- U ⇒ excessively high values of the flow speed translate into high pressure drops and a higher probability of cavitation where the duct geometrical properties vary abruptly; vibrations in the pipe can also build up. On the other side however, low values of U do not provide efficient convective heat transfer and lead to problems with removal of air bubbles at start-up. The Reynolds number is the key parameter for determining the right balance between these two conflicting requirements.
- M ⇒ chiller size is proportional to mass flow.
- T_{wall} ⇒ lower values lead to lower working temperature for the chips and the silicon sensors
- h_c ⇒ higher values indicate more efficient convection[1].
- Re ⇒ since the convective mechanism relies on molecular mixing, and this is higher in turbulent flows than in the laminar regime (where the conduction is the predominant mechanism for the heat transfer to take place), relatively high values of Re are to be preferred.
- Nu, Pr ⇒ high values of Nu as well as of Pr are to be pursued. That yields high film coefficients.

The coolants analyzed are:

- Dowcal 10, ethylene glycol based, Dow Chemical Corporation
- Dowcal N and Dowcal 20, propylene glycol based, Dow Chemical Corporation
- Syltherm XLT, Dow Chemical Corporation
- 3M Fluorinert FC-77, C_6F_{14} (FC-72) and C_8F_{18}, perfluorocarbon liquids, 3M Corporation

4.2. Results

In Figure 9 through Figure 12 data are presented. It appears that the fluorinert C_6F_{14} exhibits the best performance. This, together with the good radiation hardness shown by this fluid (ref.1), makes it a good candidate for a cooling system.

[1] Higher heat transfer coefficients imply a larger fraction of fluid participating to the heat transfer, which means that less fluid mass is being circulated through the line uselessly.

Finally, considering that the case where the pressure drop is set represents the most likely situation in our experiment. The values of T_{wall} = -5 °C and h_c = 1855 W/m^{2}K for C_6F_{14} are very close to what was assumed in the finite element model, confirming that the temperature distributions summarized in Table 2 are achievable.

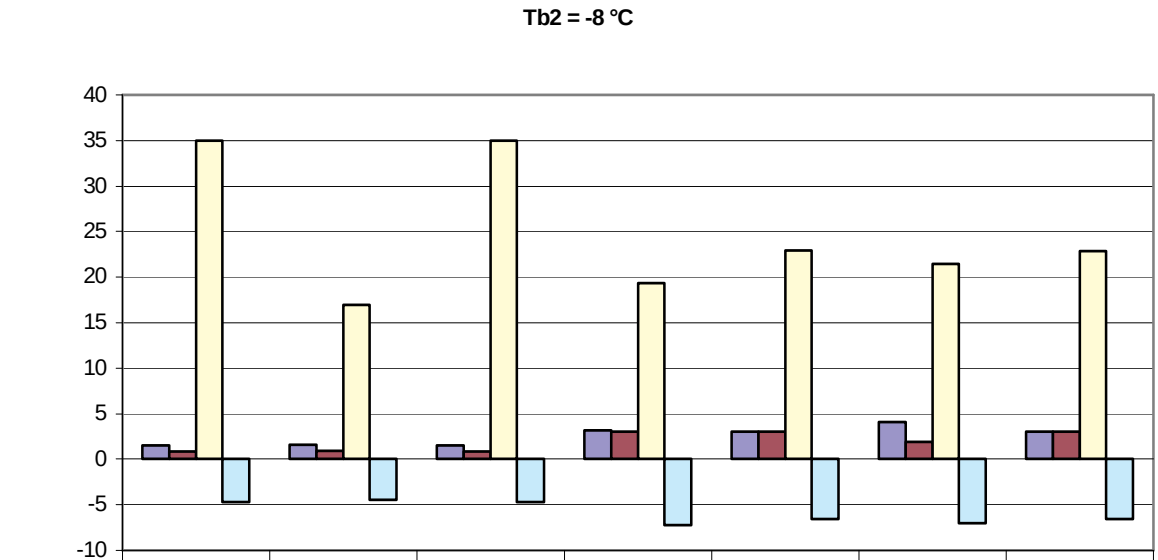

	DOWCAL N	DOWCAL 10	DOWCAL 20	C6F14	C8F18	SYLTHERM	3M FC-77
U m/s	1.542	1.621	1.542	3.185	3.02	4.093	3.019
M kg/min	0.866	0.931	0.866	3	3.001	1.903	3
DP psi	34.974	16.93	34.974	19.368	22.901	21.469	22.862
Twall °C	-4.664	-4.447	-4.721	-7.211	-6.577	-7.024	-6.577

Figure 9 – Velocity (U), mass rate (M), pressure drop (DP) and temperature at the wall (Twall) given the bulk temperature at the pipe exit.

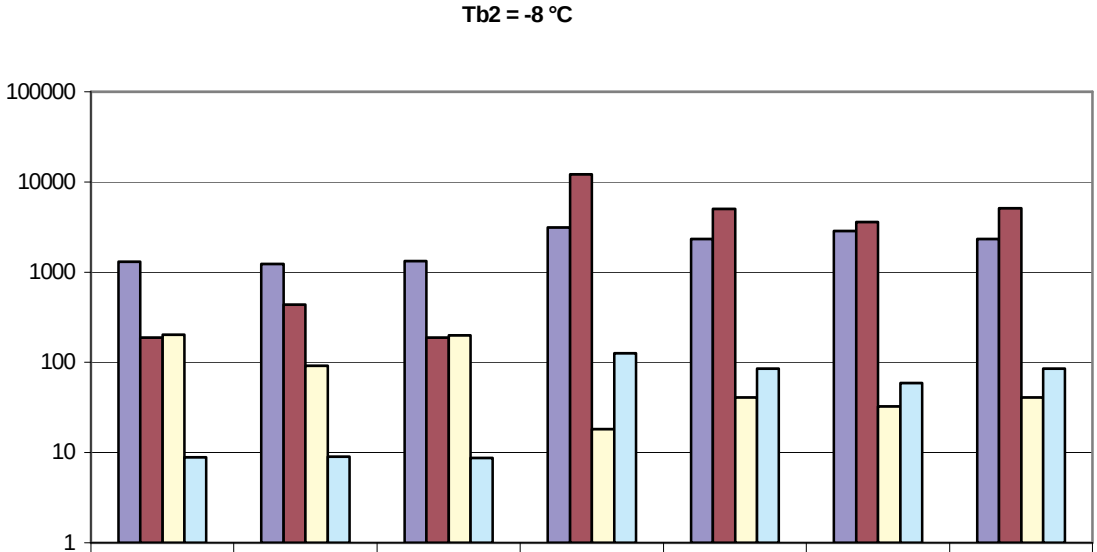

	DOWCAL N	DOWCAL 10	DOWCAL 20	C6F14	C8F18	SYLTHERM	3M FC-77
hc W/m^2 K	1304.709	1242.445	1321.863	3162.169	2334.457	2862.41	2334.633
Re -	187.438	437.614	187.438	12234.257	5070.748	3577.449	5091.794
Pr -	201.674	92.176	197.302	18.318	40.631	32.555	40.57
Nu -	8.782	8.924	8.705	126.186	85.642	59.36	85.875

Figure 10 – Film coefficient (hc), Reynolds number (Re), Prandtl number (Pr) and Nusselt number (Nu) given the bulk temperature at the pipe exit.

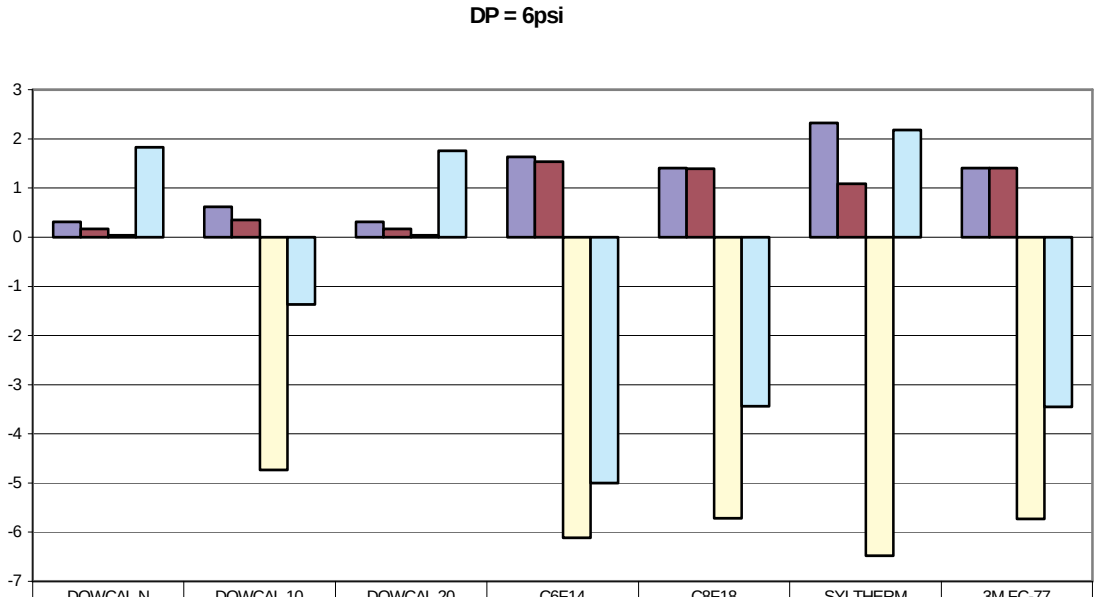

	DOWCAL N	DOWCAL 10	DOWCAL 20	C6F14	C8F18	SYLTHERM	3M FC-77
U m/s	0.306	0.614	0.306	1.635	1.412	2.324	1.414
M kg/min	0.172	0.353	0.172	1.538	1.401	1.079	1.403
Tb2 °C	0.04	-4.729	0.04	-6.106	-5.723	-6.48	-5.73
Twall °C	1.827	-1.371	1.755	-5.003	-3.433	2.189	-3.452

Figure 11 - Velocity (U), mass rate (M), exit bulk temperature (Tb2) and temperature at the wall (Twall) given the pressure drop along the pipe.

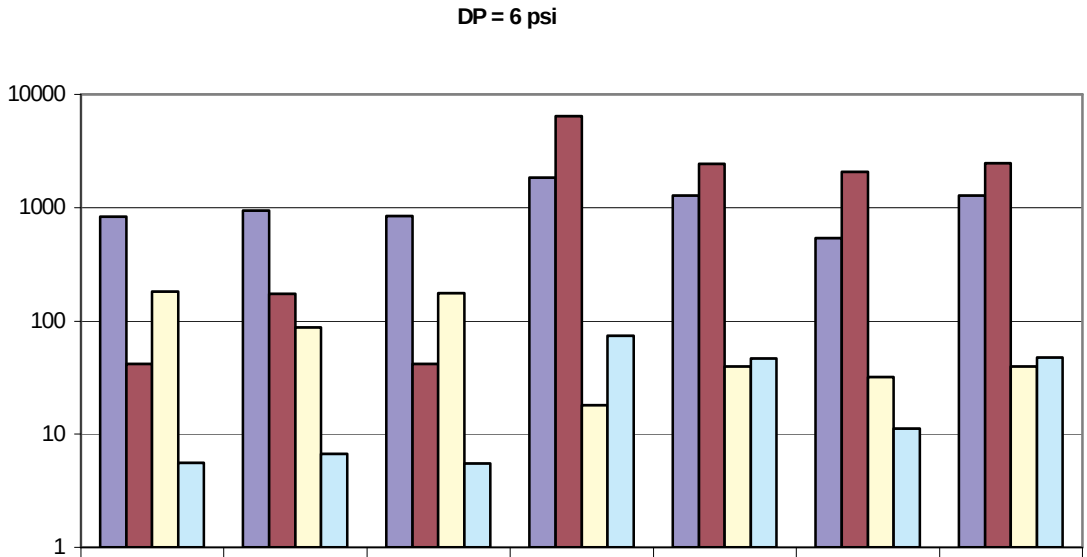

	DOWCAL N	DOWCAL 10	DOWCAL 20	C6F14	C8F18	SYLTHERM	3M FC-77
hc W/m^2 K	830.969	943.815	839.925	1854.759	1277.227	542.403	1281.7
Re -	41.634	172.763	41.634	6383.86	2438.324	2060.855	2463.693
Pr -	180.581	87.929	177.122	18.136	39.584	32.159	39.327
Nu -	5.585	6.728	5.537	74.453	46.941	11.267	47.21

Figure 12 - Film coefficient (hc), Reynolds number (Re), Prandtl number (Pr) and Nusselt number (Nu) given the pressure drop along the pipe.

4.3. The program for the coolant performance

The fluid analyses were performed using MathCAD. For brevity only the program list related to the C_6F_{14} is reported. Analogous printouts are available for the other fluids studied.

The following analysis applies to a pipe with a rectangular section. Both the laminar and the turbulent flow are predicted.

- **Given Tb2**

$Tb_1 := 263 \cdot K$

$Tb_2 := 265 \cdot K$

average bulk temperature along the pipe

$$Tb := \frac{\left(Tb_1 + Tb_2\right)}{2}$$

pipe length

$L := 1.2 \cdot m$

power to dissipate

$q_c := 100 \cdot W$

pipe inner dimensions

$b := .23 \cdot in$

$h := 0.06 \cdot in$

Geometric quantities

$A_{cross} := b \cdot h$

$p := 2 \cdot (b + h)$

$D_H := 4 \cdot \frac{A_{cross}}{p}$

Physical Properties

$$data := \begin{bmatrix} -30 & 967.38 \\ -20 & 982.92 \\ -10 & 998.46 \\ 0 & 1014.0 \\ 10 & 1029.54 \\ 20 & 1045.08 \end{bmatrix}$$

$data := csort(data, 1)$

$X := data^{<1>}$

$Y := data^{<2>}$

$S := cspline(X, Y)$

$Cpp(T) := interp\left[S, X, Y, \left(\frac{T}{K} - 273\right)\right] \cdot \frac{joule}{kg \cdot K}$

$Cp := Cpp(Tb)$

$$data := \begin{bmatrix} -30 & 0 \\ -20 & 0.0622 \\ -10 & 0.0611 \\ 0 & 0.06 \\ 10 & 0.0589 \\ 20 & 0.0578 \end{bmatrix}$$

$data := csort(data, 1)$

$X := data^{<1>}$

$Y := data^{<2>}$

$S := cspline(X, Y)$

$$kk(T) := interp\left[S, X, Y, \left(\frac{T}{K} - 273\right)\right] \cdot \frac{W}{m \cdot K}$$

$$k := kk(Tb)$$

$$data := \begin{bmatrix} -30 & 1818.3 \\ -20 & 1792.20 \\ -10 & 1766.1 \\ 0 & 1740 \\ 10 & 1713.9 \\ 20 & 1687.8 \end{bmatrix}$$

$$data := csort(data, 1)$$

$$X := data^{<1>}$$

$$Y := data^{<2>}$$

$$S := cspline(X, Y)$$

$$\rho\rho(T) := interp\left[S, X, Y, \left(\frac{T}{K} - 273\right)\right] \cdot \frac{kg}{m^3}$$

$$\rho := \rho\rho(Tb)$$

$$data := \begin{bmatrix} -30 & 1.70078 \\ -20 & 1.37287 \\ -10 & 1.13034 \\ 0 & 0.94598 \\ 10 & 0.80293 \\ 20 & 0.69016 \end{bmatrix}$$

$$data := csort(data, 1)$$

$$X := data^{<1>}$$

$$Y := data^{<2>}$$

$$S := cspline(X, Y)$$

$$\mu\mu(T) := interp\left[S, X, Y, \left(\frac{T}{K} - 273\right)\right] \cdot \frac{poise}{100}$$

$$\mu := \mu\mu(Tb)$$

$$\mu = 1.11 \cdot \frac{poise}{100}$$

flow average velocity and mass rate

$$U := 1 \cdot \frac{m}{s}$$

$$U := root\left[\left(\rho \cdot U \cdot A_{cross}\right) \cdot Cp \cdot \left(Tb_2 - Tb_1\right) - q_c, U\right]$$

$U = 3.185\ m \cdot \frac{1}{s}$

$M := \rho \cdot U \cdot A_{cross}$

$M = 3\ kg \cdot \frac{1}{min}$

Reynolds number, friction coefficient, Prandtl number, pressure loss

$Re := \rho \cdot U \cdot \frac{D_H}{\mu}$

$Re = 12234.257$

f correction factor for laminar friction coefficient in presence of rectangular cross section

$$fi := \begin{bmatrix} 0 & 1.5 \\ 0.1 & 1.34 \\ 0.3 & 1.10 \\ 0.5 & 0.97 \\ 0.8 & 0.9 \\ 1 & 0.88 \end{bmatrix}$$

$fi := csort(fi, 1)$

$X := fi^{\langle 1 \rangle}$

$Y := fi^{\langle 2 \rangle}$

$S := cspline(X, Y)$

$\phi(x) := interp(S, X, Y, x)$

$\phi := \phi\left(\frac{h}{b}\right)$

$\phi = 1.138$

$$f := \begin{cases} \left[\frac{0.3164}{(Re)^{0.25}}\right] & \text{if } \left(2320 < Re \le 10^5\right) \quad \text{(Blasius)} \\ \left(0.184 \cdot Re^{-0.2}\right) & \text{if } 10^5 < Re < 10^6 \\ \left(\phi \cdot \frac{64}{Re}\right) & \text{if } Re \le 2320 \\ \left(0.032 + 0.221 \cdot Re^{-0.237}\right) & \text{otherwise} \quad \text{(Nikuradse)} \end{cases}$$

$f = 0.03$

$f_0 := f$

$$Pr := Cp \cdot \frac{\mu}{k}$$

$Pr = 18.318$

$$\Delta p := f \cdot \frac{L}{D_H} \cdot \frac{1}{2} \cdot \rho \cdot U^2$$

$\Delta p = 19.368 \cdot psi$

Wall temperature

$$Nu(T_w) := \begin{cases} \left[0.021 \cdot Re^{0.8} \cdot Pr^{0.4} \cdot \left(\frac{T_w}{Tb} \right)^{-0.7} \cdot \left[1 + \left(\frac{L}{D_H} \right)^{-0.7} \cdot \left(\frac{T_w}{Tb} \right) \right] \right] & \text{if } Re > 2320 \quad \text{Perkins (turbulent)} \\ \left[1.86 \cdot \left(\frac{Re \cdot Pr \cdot D_H}{L} \right)^{0.33} \cdot \left(\frac{\mu\mu(Tb)}{\mu\mu(T_w)} \right) \right] & \text{otherwise} \quad \text{Sieder-Tate (laminar)} \end{cases}$$

$$hc(T_w) := k \cdot \frac{Nu(T_w)}{D_H}$$

$T_w := 273 \cdot K$

$T_{wall} := root\left[\left[hc(T_w) \cdot p \cdot L \cdot (T_w - Tb) - q_c \right], T_w \right]$

$T_{wall} = 265.789\ K$

$Tb_1 = 263\ K$

$Tb_2 = 265\ K$

$hc(T_{wall}) = 3162.169 \cdot \frac{1}{m^2 \cdot K} \cdot W$

$Nu(T_{wall}) = 126.186$

- **Given Δp**

$\Delta p := 6 \cdot psi$

$Tb_2 :=$ | $Tb \leftarrow Tb_1$

$f \leftarrow f_0$

$Uref \leftarrow 1 \cdot \frac{m}{s}$

$Cp \leftarrow Cpp(Tb)$

$k \leftarrow kk(Tb)$

$\rho \leftarrow \rho\rho(Tb)$

$\mu \leftarrow \mu\mu(Tb)$

for $i \in 1 .. 5$

$x \leftarrow 1 \cdot \frac{m}{s}$

$U \leftarrow root\left[\left(\Delta p - f \cdot \frac{L}{D_H} \cdot \frac{1}{2} \cdot \rho \cdot x^2\right), x\right]$

break if $|U - Uref| < 0.001 \cdot \frac{m}{s}$

$Uref \leftarrow U$

$Tx \leftarrow 273 \cdot K$

$Tb_2 \leftarrow root\left[q_c - \rho \cdot U \cdot A_{cross} \cdot Cp \cdot \left(Tx - Tb_1\right), Tx\right]$

$Tref \leftarrow Tb_2$

$Tb \leftarrow \frac{Tb_1 + Tb_2}{2}$

$Cp \leftarrow Cpp(Tb)$

$k \leftarrow kk(Tb)$

$\rho \leftarrow \rho\rho(Tb)$

$\mu \leftarrow \mu\mu(Tb)$

$Re \leftarrow \rho \cdot U \cdot \frac{D_H}{\mu}$

$f \leftarrow$ | $\frac{0.3164}{(Re)^{0.25}}$ if $2320 < Re \le 10^5$

$\left(0.184 \cdot Re^{-0.2}\right)$ if $10^5 < Re < 10^6$

$\left(\phi \cdot \frac{64}{Re}\right)$ if $Re \le 2320$

$\left(0.032 + 0.221 \cdot Re^{-0.237}\right)$ otherwise

Tb_2

$Tb_2 = 266.894\ K$

$$Tb := \frac{(Tb_1 + Tb_2)}{2}$$

$Cp := Cpp(Tb)$

$k := kk(Tb)$

$\rho := \rho\rho(Tb)$

$\mu := \mu\mu(Tb)$

$U := root\left[q_c - \rho \cdot U \cdot A_{cross} \cdot Cp \cdot (Tb_2 - Tb_1), U\right]$

$U = 1.635\ \frac{m}{s}$

$M := \rho \cdot U \cdot A_{cross}$

$M = 1.538\ kg \cdot \frac{1}{min}$

$$Pr := Cp \cdot \frac{\mu}{k}$$

$$Re := \rho \cdot U \cdot \frac{D_H}{\mu}$$

$Re = 6383.86$

$Pr = 18.136$

Wall temperature

$$Nu(T_w) := \begin{cases} \left[0.021 \cdot Re^{0.8} \cdot Pr^{0.4} \cdot \left(\frac{T_w}{Tb}\right)^{-0.7} \cdot \left[1 + \left(\frac{L}{D_H}\right)^{-0.7} \cdot \left(\frac{T_w}{Tb}\right)\right]\right] & \text{if } Re > 2320 \quad \text{Perkins (turbulent)} \\ \left[1.86 \cdot \left(\frac{Re \cdot Pr \cdot D_H}{L}\right)^{0.33} \cdot \left(\frac{\mu\mu(Tb)}{\mu\mu(T_w)}\right)\right] & \text{otherwise} \quad \text{Sieder-Tate (laminar)} \end{cases}$$

$$hc(T_w) := k \cdot \frac{Nu(T_w)}{D_H}$$

$T_w := 273 \cdot K$

$T_{wall} := root\left[\left[hc(T_w) \cdot p \cdot L \cdot (T_w - Tb) - q_c\right], T_w\right]$

$T_{wall} = 267.997\ K$

$Tb_1 = 263\ K$

Tb = 264.947 K

Tb_2 = 266.894 K

$hc(T_{wall})$ = 1854.759 $\frac{1}{m^2 \cdot K} \cdot W$

$Nu(T_{wall})$ = 74.453

5. References

1. «Radiation Hardness Studies of Cooling Fluids. Epoxies and Capacitors for CMS Pixel System», M.Atac, B.Gobbi, L.Cremaldi, J.Hoffman
2. «Principles of Heat Transfer», F.Kreith, M.S.Bohn, 6th ed., Brooks/Cole
3. «Handbook of Mechanical Engineering», H.Dubbel, Hardcover, Springer-Verlag New York, Incorporated, November 1994